Determining Thresholds For Contrast Agent Collapse

Azzdine Y. Ammi, Jonathan Mamou[†], Grace I. Wang[†], Robin O. Cleveland[‡]
S. Lori Bridal, William D. O 'Brien, Jr[†]

Laboratoire d'Imagerie Paramétrique, UMR 7623 C.N.R.S.- Paris VI
[†]Bioacoustics Research Laboratory, University of Illinois at Urbana-Champaign
[‡]Dept. of Aerospace and Mechanical Engineering, Boston University

Abstract - **Determining the threshold of fragmentation of ultrasound contrast agents is important for both imaging and therapeutic ultrasound applications. We detected acoustic emissions from Optison™ microbubbles that were insonified by pulses of ultrasound. Our observations suggest that when the microbubbles rupture, daughter bubbles are created which subsequently grow and then collapse on a time-scale of 1-5 µs. The emission from the "rebound" collapse occurs after the end of the excitation pulse and we used the presence of this signal to determine the thresholds for the shell rupture. These shell-disruption thresholds were found to increase with frequency and decrease with pulse length.**

I. Introduction

Ultrasonic contrast agents consist of small stabilized microbubbles (< 10 µm diameter) that are injected vascularly to enhance contrast and enable nonlinear imaging capabilities. Enhanced sonographic contrast improves early detection of a variety of disease processes including heart disease and cancer [1, 2].

A multitude of novel imaging techniques detecting nonlinear microbubble oscillations, echo decorrelation during microbubble destruction or the rate at which vascularized zones fill with contrast have been proposed [3]. Microbubbles also offer promise as vectors to carry encapsulated medicines to a targeted treatment site with delivery initiated by ultrasonic destruction of the bubble capsule [4]. Successful and reproducible applications of such exciting techniques require that the interaction of the ultrasound wave with the microbubble be optimized and well controlled. Furthermore, questions concerning the potential bioeffects of microbubble destruction need to be addressed to assure safety [5, 6].

Thus, researchers have begun to study collapse thresholds of contrast microbubbles and to develop models to predict collapse thresholds based on contrast agent properties (e.g.,. composition of encapsulating shell, gas, size distribution). Chen et al [7] used detection of broadband noise from ensembles of insonified microbubbles in suspension to determine fragmentation thresholds for four contrast agents (at 1.1 and 3.5 MHz). Chomas et al [8] used a high-speed camera to observe acoustic contrast destruction in isolated experimental contrast agent microbubbles. In particular, their work explores the dependence of fragmentation threshold on excitation pulse parameters.

This work characterizes collapse thresholds experimentally for a widely used commercial agent (Optison™) over a range of acoustic pressures (0.2 to 5 MPa) at 3 frequencies (1, 3 and 5 MHz) and 3 pulse durations (3, 5 and 7 cycles). By using highly diluted contrast suspensions, sensitive detectors and a unique acoustic signature for microbubble collapse, the passive cavitation approach used in this study allows the detection of the collapse of single microbubbles without calling upon optical observation.

II. Materials and Method

Contrast agent

Experiments were conducted using Optison™, an FDA-approved contrast agent solution. Microbubbles have a mean diameter in the range of 2-4.5 µm and an albumin shell containing perflutren C_3F_6 gas [9]. The solution in the vial has a concentration in the range of 5 to 8×10^8 microbubbles/mL.

Passive cavitation detector

Measurements were made in a tank containing 9.6 ± 0.3 L of degassed water between 20 and 22°C. A single-element (either 1, 3 or 5 MHz center-frequency) focused transducer was used to insonify the bubbles. A 15 MHz focused transducer, (mounted confocal and at a 70° angle to the transmitter) was used to collect emissions from the bubbles. Transducer characteristics are summarized in Table I. A diagram of the set-up is shown in Figure 1.

The pressure waveform obtained at the focus of each emitting transducer (for each setting used in the experiments) was measured using a Marconi hydrophone (Type 699). The -6 dB field limits were determined for each transducer, in a pulse-echo configuration, by measuring the scattered signal from a wire reflector translated throughout the focal region. When transducers were aligned at 70°, and the receiver's -6 dB field limits were fully inside the –6 dB limits of the emitter. Thus the active, confocal area corresponded to the 15 MHz transducer's – 6 dB field limits: a cigar-shaped volume 3400 µm long and 262 µm in diameter (approximate volume of 0.12 mm^3).

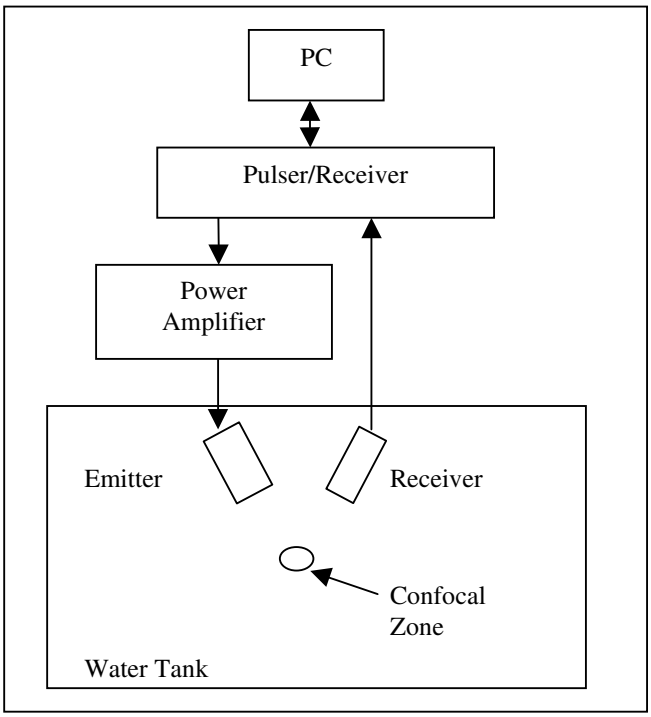

Figure 1: Experimental configuration of the passive cavitation detector.

For each experiment 0.2-mL of Optison™ was injected into the tank. This corresponds to approximately 10^8 microbubbles and resulted in a mean concentration in the tank of about 10 bubbles/µL. Thus, on average, only 1 microbubble should be within the 6-dB receiver volume.

The water was gently stirred with a pump to distribute the agent and replenish contrast in the active volume. Sinusoidal tone bursts were sent by the emitting transducer for a selected combination of amplitude (0.2 to 5 MPa, in steps of ~0.07 MPa) and number of cycles (3, 5 or 7). Pulse phase was kept at 0° and PRF at 10 Hz for all measurements. The 15 MHz transducer passively received signals favorizing reception of signals in its useful bandwidth, above the transmit frequency range. The output of the receiver (Ritec Advanced Measurement System RAM 5000) was amplified at 44 dB. For each set of emission settings, 128 consecutive received waveforms were recorded by a digitizing board (Strategic Test UF 3025, 12-bit, 200 MHz). It was verified that no signals above the noise level were received in the absence of Optison™.

TABLE I
MEASURED TRANSDUCER CHARACTERISTICS.
NOMINAL CENTER FREQUENCIES: 1, 3, 5 AND 15 MHz (F#2).

Center frequency (MHz)	-6 dB bandwidth (MHz)	Focal distance (cm)
0.9	0.8-1.0	3.81
2.8	2.6 - 3.0	3.81
4.6	4.3 - 4.8	3.81
13	9.3 - 17.6	1.54

Data analysis

Each recorded waveform was evaluated for the presence or absence of received signals above the noise level. Only waveforms with signals above a threshold, indicating the presence of a microbubble, were selected for further analysis. A sliding Blackman window (120 points, 0.6 µs) was moved along the selected portion of each time-trace with steps of 0.025 µs, and the fast Fourier transform (FFT) was calculated, yielding the received spectrum as a function of time and frequency.

III. Results

Fig. 2 presents a representative echo waveform and the associated time-frequency spectrogram measured by the 15 MHz receiver for the case of a collapsing single microbubble. The excitation pulse was a 5 MHz, 7-cycle burst with a peak rarefactional pressure of 1 MPa.

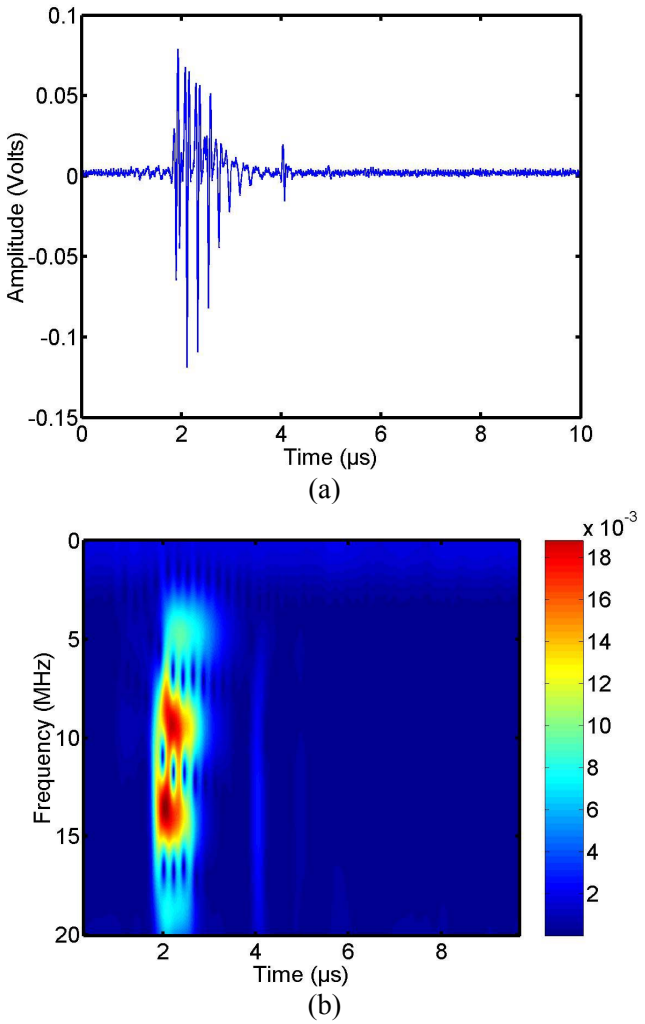

Figure 2: Results obtained for a 5MHz, 7-cycle, 1 MPa excitation (a)Waveform detected with a 15 MHz receiver. (b) Corresponding time-frequency spectrogram

The signal between approximately 2 and 3 μs corresponds to the response of the microbubble due to the excitation. In the spectrogram the strong bands near 10 and 15 MHz are harmonics generated both by nonlinear propagation distortion of the incident pulse and nonlinear bubble dynamics. The four thin vertical lines in the spectrogram are the wideband emission from collapses of the microbubble. After the end of the excitation, at around 4 μs, a short pulse can be seen in the time trace and a corresponding broadband signature (from 5 to 20 MHz) can be observed in the spectrogram. We interpret this signal as the "rebound" collapse of daughter bubbles indicating the detection of a collapse event. These daughter bubbles are released once the shell has ruptured and have been observed optically by Chomas et al [10] .We speculate that the unconstrained daughter bubbles are able to grow and collapse essentially as free inertial cavitation bubbles [11]. It is highly unlikely that the rebound signature could be generated by a bubble that is still encapsulated because encapsulated bubble oscillations are damped by the shell properties after the excitation.

We note also in Fig. 2 that there is evidence of a second rebound at 5 μs—an event which is also consistent with the existence of a free bubble undergoing inertial oscillations. Therefore we used the presence of the "rebound" collapse to define a rupture threshold for the microbubble: the lowest peak rarefactional excitation pressure for which a rebound is detected on any of the acquired waveforms.

Figure 3 shows the peak positive and negative voltages from the 15 MHz cavitation detector as a function of the peak rarefactional excitation pressure. Data is shown for 3, 5 and 7 cycle pulses of 5-MHz ultrasound with a 10 Hz PRF. Each point is the average value from the subset of the 128 acquired time traces where an event was detected (standard deviations are represented by the error bars).

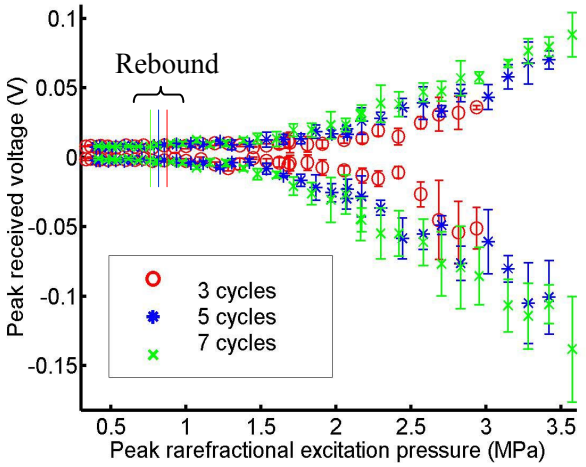

Figure 3 : Peak positive and negative voltage measured by the 15 MHz receiver as a function of peak rarefactional pressure for bubbles excited with a 5 MHz burst.

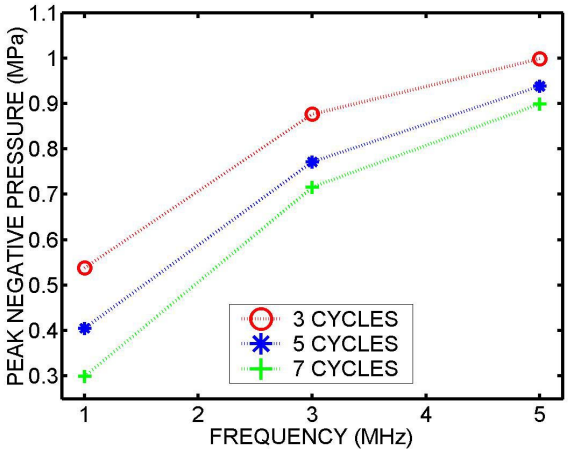

Figure 4: Collapse thresholds obtained using rebound signals.

For incident pressures up to about 1.5 MPa, there is a smooth increase in the peak received signal. However for peak negative pressures above 1.5 MPa there is a marked increase in the standard deviation of the echoes' signals which can be attributed to large variations in the pulse-to-pulse response of the microbubbles—presumably due to rupture of the contrast agents.

The vertical colored lines represent the incident peak negative pressure thresholds at which the first rebound pulse was detected for each pulse length. We note that the rebound signals were detected for peak rarefractional pressures around 0.8 MPa well below the onset of unsteady behaviour of the peak voltages. Thus, occurrence of rebound signals appears to be a more sensitive predictor of contrast agent rupture than the modification of detected echo amplitudes which has been used in other studies [7].

In Fig. 4 the lowest peak rarefactional excitation pressures for which rebound pulses were observed in the detected data are plotted as a function of the center frequency and the number of cycles of the excitation pulse (PRF 10 Hz). The data show that as frequency was increased the peak negative pressure required to initiate rupture increased. The data also show that as the number of cycles was increased the peak negative pressure required for rupture decreased.

IV. Discussion

Using a passive cavitation detector, we have identified a signature in the signal from ultrasound contrast agent microbubbles that appears to be a unique identifier of contrast agent rupture. We contend that once a contrast agent has ruptured during excitation, daughter bubbles of interior gas are liberated which can undergo unconstrained inertial cavitation on time scales beyond the excitation pulse. We found that the subsequent "rebound" collapse of the daughter bubbles occurred a few microseconds after excitation ceased and resulted in the emission of a short broadband pulse. The presence of the rebound signal was detected at delays of up to 4 μs and in some cases multiple rebounds were detected.

Because the rebound signal was separated in time from the main echo it was easily distinguished from the other responses of the bubble and consequently appears to be a more sensitive detector of contrast agent rupture than the main echo received from the excitation signal. This is because the main echo signal contains spectral components from many sources, for example, nonlinear propagation of the incident pressure pulse and nonlinear bubble dynamics.

Based on identification of the rebound signal we determined thresholds in terms of frequency (1, 3 or 5 MHz), pulse duration (3, 5 or 7 cycles) and peak rarefactional pressure. The thresholds varied from 0.3 to 1 MPa. For a 1 MHz, 7 cycle pulse (PRF 10 Hz), we found the collapse threshold of Optison™ to be 0.29 MPa. This compares favorably with the value of 0.13 MPa for a longer pulse (10 cycles at 1.1 MHz) reported by Chen et al [6], who used broadband noise to identify destruction thresholds.

We found that the peak negative excitation pressure necessary to induce rupture increased with the frequency of the excitation. This result was expected as at lower frequencies the duration of the negative pressure (which drives the microbubble growth) is longer and should therefore make bubbles grow to a larger size that is more likely to provoke shell failure. Also we found that shorter pulses required larger peak negative pressures to induce rupture. This is also expected as rupture in most materials is a stochastic process and therefore by applying more cycles per pulse one is more likely to rupture the shell.

IV. Conclusions

In this work, we have acoustically investigated the rupture pressure thresholds of single shelled-microbubbles of Optison™ as a function of excitation pulse frequency and duration. It has been already shown with optical observations that microbubble rupture is followed by the creation of unshelled daughter bubbles [10]. We identified the emitted signal corresponding to the 'rebound' collapse of these bubbles. These rebounds are broadband and occur well after acoustic excitation has ceased. Thresholds measured based on lowest rarefactional pressure at which rebound was observed are consistent with results reported for similar shelled agents but based on optical or broadband-noise detection techniques [7, 8]. Because the rebound signal is not subject to non linear propagation and bubble oscillation spectral components present in the echo received in response to excitation, it appears to provide a straight-forward and sensitive approach for determining contrast agent rupture thresholds.

References

[1] H. Fujii, S. Tomita, T. Nakatani, S. Fukuhara, A. Hanatani, Y. Ohtsu, M. Ishida, C. Yutani, K. Miyatake, and S. Kitamura, "A novel application of myocardial contrast echocardiography to evaluate angiogenesis by autologous bone marrow cell transplantation in chronic ischemic pig model," *J Am Coll Cardiol*, vol. 43, pp. 1299-1305., 2004.

[2] V. Migaleddu, G. Virgilio, D. Turilli, M. Conti, G. Campisi, N. Canu, D. Sirigu, and I. Vincentelli, "Characterization of focal liver lesions in real time using harmonic imaging with high mechanical index and contrast agent levovist," *AJR Am J Roentgenol*, vol. 182, pp. 1505-1512., 2004.

[3] J. Eyding, W. Wilkening, M. Reckhardt, G. Schmid, S. Meves, H. Ermert, H. Przuntek, and T. Postert, "Contrast burst depletion imaging (CODIM): a new imaging procedure and analysis method for semiquantitative ultrasonic perfusion imaging," *Stroke*, vol. 34, pp. 77-83., 2003.

[4] R. V. Shohet, S. Chen, Y. T. Zhou, Z. Wang, R. S. Meidell, R. H. Unger, and P. A. Grayburn, "Echocardiographic destruction of albumin microbubbles directs gene delivery to the myocardium," *Circulation*, vol. 101, pp. 2554-2556., 2000.

[5] E. Stride and N. Saffari, "The potential for thermal damage posed by microbubble ultrasound contrast agents," *Ultrasonics*, vol. 42, pp. 907-913., 2004.

[6] J. F. Zachary, S. A. Hartleben, L. A. Frizzell, and W. D. O'Brien, Jr., "Arrhythmias in rat hearts exposed to pulsed ultrasound after intravenous injection of a contrast agent," *J Ultrasound Med*, vol. 21, pp. 1347-1356; discussion 1343-1345., 2002.

[7] W. S. Chen, T. J. Matula, A. A. Brayman, and L. A. Crum, "A comparison of the fragmentation thresholds and inertial cavitation doses of different ultrasound contrast agents," *J Acoust Soc Am*, vol. 113, pp. 643-651., 2003.

[8] J. E. Chomas, P. Dayton, D. May, and K. Ferrara, "Threshold of fragmentation for ultrasonic contrast agents," *J Biomed Opt*, vol. 6, pp. 141-150., 2001.

[9] S. Podell, C. Burrascano, M. Gaal, B. Golec, J. Maniquis, and P. Mehlhaff, "Physical and biochemical stability of Optison, an injectable ultrasound contrast agent," *Biotechnol Appl Biochem*, vol. 30, pp. 213-223., 1999.

[10] J. E. Chomas, P. Dayton, J. Allen, K. Morgan, and K. W. Ferrara, "Mechanisms of contrast agent destruction," *IEEE Trans Ultrason Ferroelectr Freq Control*, vol. 48, pp. 232-248., 2001.

[11] S. L. Ceccio and C. E. Brenne, "Observation of the dynamics and acoustics of travelling bubble cavitation," *J. Fluid Mech*, vol. 233, pp. 633-660., 1991.